Simple membrane-based model of the Min oscillator

2015 New J. Phys. 17 043023

(http://iopscience.iop.org/1367-2630/17/4/043023)

IOP Publishing New J. Phys. 17 (2015) 043023 doi:10.1088/1367-2630/17/4/043023

New Journal of Physics
The open access journal at the forefront of physics

Deutsche Physikalische Gesellschaft DPG
IOP Institute of Physics

Published in partnership with: Deutsche Physikalische Gesellschaft and the Institute of Physics

OPEN ACCESS

RECEIVED
19 December 2014

REVISED
10 March 2015

ACCEPTED FOR PUBLICATION
10 March 2015

PUBLISHED
14 April 2015

PAPER

Simple membrane-based model of the Min oscillator

Zdeněk Petrášek[1,2] **and Petra Schwille**[1]

[1] Department of Cellular and Molecular Biophysics, Max-Planck-Institute of Biochemistry, Am Klopferspitz 18, 82152 Martinsried, Germany
[2] Institut für Biotechnologie und Bioprozesstechnik, Technische Universität Graz, Petersgasse 10-12/I, 8010 Graz, Austria

E-mail: z.petrasek@tugraz.at

Keywords: Min oscillations, pattern formation, self-organization, dynamic instability

Abstract

Min proteins in *E. coli* bacteria organize into a dynamic pattern oscillating between the two cell poles. This process identifies the middle of the cell and enables symmetric cell division. In an experimental model system consisting of a flat membrane with effectively infinite supply of proteins and energy source, the Min proteins assemble into travelling waves. Here we propose a simple one-dimensional model of the Min dynamics that, unlike the existing models, reproduces the sharp decrease of Min concentration when the majority of protein detaches from the membrane, and even the narrow MinE maximum immediately preceding the detachment. The proposed model thus provides a possible mechanism for the formation of the MinE ring known from cells. The model is restricted to one dimension, with protein interactions described by chemical kinetics allowing at most bimolecular reactions, and explicitly considering only three, membrane-bound, species. The bulk solution above the membrane is approximated as being well-mixed, with constant concentrations of all species. Unlike other models, our proposal does not require autocatalytic binding of MinD to the membrane. Instead, it is assumed that two MinE molecules are necessary to induce the dissociation of the MinD dimer and its subsequent detachment from the membrane. We investigate which reaction schemes lead to unstable homogeneous steady states and limit cycle oscillations, and how diffusion affects their stability. The suggested model qualitatively describes the shape of the Min waves observed on flat membranes, and agrees with the experimental dependence of the wave period on the MinE concentration. These results highlight the importance of MinE presence on the membrane without being bound to MinD, and of the reactions of Min proteins on the membrane.

Introduction

The combination of chemical reactions with diffusion under non-equilibrium conditions can give rise to a range of complex phenomena, such as formation of steady patterns, travelling waves or periodic oscillations [1–3]. The resulting patterns and structures often have spatial dimensions exceeding the molecular size by many orders of magnitude, and temporal periods much longer than the time scales of the underlying chemical reactions. Still, their size and dynamics are precisely determined by the parameters describing the interactions and motion of individual molecules.

These self-organizing physico-chemical phenomena are important for the functioning of living matter, as they provide accurate 'rulers' and 'clocks' that then determine the size and dynamics of the whole organism or its part [4–6]. Most prominent examples include spatial gradients of molecular concentrations that control the growth and development of cells, embryos and tissues [7–9], and temporal concentration oscillations forming the basis of circadian rhythms that adjust the functioning of an organism to the day/night cycle [10, 11].

The Min proteins in the rod-like *E. coli* bacteria bind to the inner membrane surface, where they organize into a dynamic pattern oscillating between the two cell poles. The resulting exclusion of one of the proteins, MinC, from the cell center is important for accurate positioning of the cell division ring and for symmetric cell division [12]. The Min system consists of three proteins: MinD, MinE and MinC, but only the first two are

necessary for the oscillations. Although many details of the interaction of Min proteins with the membrane and among themselves are known [12, 13], the exact mechanism of the oscillations is not yet fully understood.

An important step towards the understanding of the Min dynamics was the observation of dynamic Min patterns on artificially created supported lipid bilayers [14–16], on structured membrane surfaces [17], on unsupported lipid membranes [18], and within microcompartments enclosing a small volume [19]. These synthetic systems allow easier control of all relevant parameters, such as protein concentration, membrane composition and volume geometry, and so enable quantitative studies of their effect on the Min pattern dynamics.

The models of Min oscillations are usually based on the reaction–diffusion mechanism. The steady state of the reaction system is unstable, which leads to inhomogeneous oscillating protein distribution. The early models employed effective reaction terms [20, 21] or included effective processes such as aggregation current describing the tendency of MinD to aggregate on the membrane [22–24]. Although the introduction of sufficient non-linearity in the rate equations in these models results in instability and complex dynamics, it does not always allow a direct interpretation in terms of biochemical reactions.

A clear interpretation is possible with models containing only terms describing simple reaction steps. While some models contain cubic terms corresponding to non-realistic trimolecular reactions [14], other models employ only at most bimolecular reactions [16, 25–28]. Several other models attempt to explain the Min dynamics by relying on the observed MinD polymerization into filaments [29], often combined with preferential nucleation at the cell poles [30–32].

There are two classes of models that are relatively simple, contain only chemical reaction terms, make minimum assumptions beyond firmly established facts, and exhibit Min dynamics similar to those in cells or flat membranes. In the first of them, the finite rate of conversion of MinD–ADP, which cannot bind to the membrane, to the MinD–ATP in the bulk solution plays an important role [25, 28]. In the other class of models, the existence of MinE not attached to MinD on the membrane is important, and the reactions in the bulk are not considered (i.e. are assumed to proceed fast) [16, 27].

Here we propose a model related to the second type. Contrary to most other models, the model we suggest does not require autocatalytic binding of MinD to the membrane. Instead, it assumes that two MinE molecules are necessary to induce MinD detachment from the membrane. This assumption is based on MinD being a dimer with two binding sites for MinE and two bound ATP molecules. The model is very simple, not far from (in terms of complexity) the minimal chemical model that can exhibit instability and periodic oscillations [33]. It includes only reactions on the membrane and explicitly contains only three, membrane-bound, species. In comparison to other models, it provides so far the best qualitative description of the shapes of the observed *invitro* concentration profiles of MinE on lipid bilayers, and reproduces the experimental dependence of the wave period on the MinE concentration.

We first study the dynamical behaviour and stability of this model considered as a well-mixed system, neglecting diffusion. We explore modifications of the model concerning the way of attachment of MinE to the membrane and the necessity of two MinE molecules for MinD membrane detachment. Then we add diffusion and observe its effects on the wave shape and propagation. Finally, we briefly consider this model in closed geometry with a finite pool of MinD and MinE molecules.

Results

The model

To capture the essential features of the Min dynamics and pattern formation we aim to keep the model as simple as possible. This means using small number of species and reactions, and a simple geometry of the reaction domain.

The two proteins, MinD and MinE, are necessary and sufficient to produce the dynamic patterns on lipid bilayers. The following experimental facts concerning their interactions are generally accepted: MinD in its ATP-form binds to the membrane [34]; once bound, it strongly enhances binding of MinE to the membrane [35, 36]; and MinE on the membrane stimulates the ATP-ase activity of membrane-bound MinD, leading to the release of both MinD and MinE from the membrane [35, 37].

These facts are usually incorporated into the kinetic models in form of the following three reactions: MinD binds to the membrane resulting in membrane-bound MinD species; MinE binds to MinD on the membrane, forming a MinD–MinE membrane-bound complex, and MinD–MinE complex dissociates (following ATP hydrolysis) and leaves the membrane. These reactions alone, if assumed to take place in their simplest form, are not sufficient to make the steady state of the system unstable, and no interesting behaviour, such as oscillations or creation of patterns, takes place. A certain increase in complexity is therefore necessary.

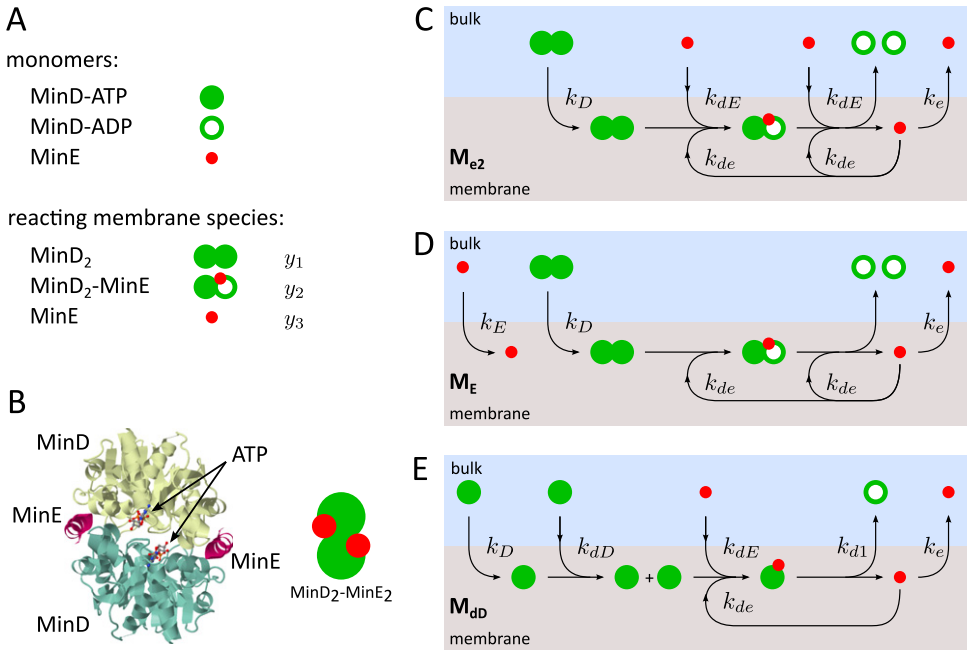

Figure 1. Models of MinD and MinE membrane interactions. A: the three monomers, MinD in the ATP- and ADP-form and MinE, are the basic units of the membrane-bound species in the models considered in this work: MinD dimer (concentration y_1), MinD dimer with one MinE bound (y_2) and MinE (y_3). B: the structure of the MinD dimer [38] with two ATP molecules at the interface between the two monomers, and the two MinE binding sites formed at the contact points of the two MinD monomers. The interacting helices of MinE are shown in red (Image from the RCSB PDB (www.rcsb.org of 3Q9L). C: the model M_{e2} based on the assumption that two MinE molecules are required for the $MinD_2$–MinE complex to dissociate and leave the membrane. D: the direct MinE attachment model M_E : analogous to M_{e2} but with direct binding of MinE to the membrane. E: the model M_{dD} with autocatalytic attachment of MinD to the membrane.

All models based on chemical kinetics (i.e. not using effective reaction terms) additionally assume enhancement of MinD binding by MinD already present on the membrane. This is typically represented as an autocatalytic term in the differential equation for the concentration c of the membrane-bound MinC of the form $\dot{c} = +kc\ldots$, where the rate constant k is a linear function of the concentration of MinD in the solution above the membrane.

The published models additionally add at least one more species, in addition to the membrane-bound MinD and MinD–MinE complex. One possibility is based on the assumption that MinE from the dissociated MinD–MinE complex stays on the membrane for a certain time during which it can bind to another MinD and form a new MinD–MinE complex [16, 27]. This idea results from experiments showing a longer residence time of individual MinE on the membrane in comparison to MinD [39], and on biochemical evidence [40].

A model combining autocatalytic MinD attachment with MinE as a third membrane-bound species (model M_{dD}) is depicted in figure 1(E). It is closely related to the models recently used to describe the Min dynamics [16, 27].

The model proposed here includes MinE as a third species, but does not require autocatalytic MinD membrane attachment. It is inspired by the fact that MinD in its ATP-form is a dimer (figure 1(B)), with the two ATP molecules at the interface between the two monomers [38]. Upon ATP hydrolysis the dimer dissociates; one can imagine that the ATP molecules act as a 'glue' holding the dimer together as long as they are not hydrolysed. The dimer has two symmetrically positioned binding sites for MinE at the interface of the two monomers. We assume that MinE binding to one binding site stimulates the ATP-ase activity of MinD, leading to hydrolysis of one of the ATP molecules. Binding of another MinE to the other symmetric site stimulates hydrolysis of the other ATP. As long as at least one ATP is not hydrolyzed, the whole complex holds together. Only after both ATP are converted to ADP, the MinD dimer dissociates, releasing also both MinE molecules since their binding sites at the MinD monomer interfaces cease to exist.

While MinD dimer is stably attached to the membrane by two membrane-targeting sequences (mts), the MinD monomer is anchored by only one mts, providing only a weak membrane affinity, and therefore dissociates from the membrane quickly.

The susequent binding of two MinE molecules to $MinD_2$ and their simultaneous release from the complex makes the reaction system sufficiently complex to exhibit instability and consequently rich dynamics. As we

show below, the requirement of two MinE molecules for the complex dissociation is not stringent, and a certain degree of the $MinD_2$–MinE complex dissociation stimulated by only one MinE can be tolerated.

Well-mixed system

First, we consider a well-mixed system: the situation where the membrane diffusion is infinitely fast and the effects of diffusion-limited mixing are neglected. The concentrations of all species y_i are then spatially homogeneous and depend only on time. Later on we will investigate the effects of finite diffusion.

The model proposed here assumes three membrane-bound species: $MinD_2$ (concentration y_1), $MinD_2$–MinE complex (y_2), and MinE (y_3). Although MinD is thought of as a dimer, the only implication of this fact is the existence of two binding sites for MinE. No MinD dimerization kinetics is included in the model.

The following reactions constitute the model (figure 1(C)): $MinD_2$ binds to the membrane (rate constant k_D); MinE binds to one of the binding sites on $MinD_2$, this being either MinE from the solution (rate constant k_{dE}) or MinE already present on the membrane (rate constant k_{de}); MinE binds to the second binding site on the $MinD_2$ (again, either MinE from the solution or from the membrane); this is followed immediately by the dissociation of the complex, and detachment of MinD from the membrane. Finally, MinE leaves the membrane with the rate constant k_e ($\varnothing$ in the following reactions stands for no membrane-bound reactants or products).

$$\varnothing \xrightarrow[k_D]{+\mathrm{MinD_2}} \mathrm{MinD_2}, \tag{1}$$

$$\mathrm{MinD_2} \xrightarrow[k_{dE}]{+\mathrm{MinE}} \mathrm{MinD_2{-}MinE}, \tag{2}$$

$$\mathrm{MinE} + \mathrm{MinD_2} \xrightarrow[k_{de}]{} \mathrm{MinD_2{-}MinE}, \tag{3}$$

$$\mathrm{MinD_2{-}MinE} \xrightarrow[k_{dE}]{+\mathrm{MinE},-\mathrm{MinD_2}} 2\ \mathrm{MinE}, \tag{4}$$

$$\mathrm{MinE} + \mathrm{MinD_2{-}MinE} \xrightarrow[k_{de}]{-\mathrm{MinD_2}} 2\ \mathrm{MinE}, \tag{5}$$

$$\mathrm{MinE} \xrightarrow[k_e]{-\mathrm{MinE}} \varnothing. \tag{6}$$

The following system of differential equations describes the dynamical system:

$$\dot{y}_1 = k_D - k_{de}\, y_1 y_3 - k_{dE}\, y_1, \tag{7}$$

$$\dot{y}_2 = k_{de}\, y_1 y_3 + k_{dE}\, y_1 - k_{de}\, y_2 y_3 - k_{dE}\, y_2, \tag{8}$$

$$\dot{y}_3 = -k_{de}\, y_1 y_3 + k_{de}\, y_2 y_3 + 2k_{dE}\, y_2 - k_e\, y_3. \tag{9}$$

It is convenient to change to non-dimensional quantities t′ and y_i' by expressing time in the units of $1/k_e$ and concentrations in the units of k_D/k_e:

$$t' = k_e\, t, \tag{10}$$

$$y_i' = \frac{k_e}{k_D} y_i. \tag{11}$$

Then we obtain (after dropping the primes of t′ and y_i') a system of equations that we will refer to as model M_{e2} (the two-step MinD dissociation model):

$$\dot{y}_1 = 1 - \kappa_{de}\, y_1 y_3 - \kappa_{dE}\, y_1, \tag{12}$$

$$\dot{y}_2 = \kappa_{de}\, y_1 y_3 + \kappa_{dE}\, y_1 - \kappa_{de}\, y_2 y_3 - \kappa_{dE}\, y_2, \tag{13}$$

$$\dot{y}_3 = -\kappa_{de}\, y_1 y_3 + \kappa_{de}\, y_2 y_3 + 2\kappa_{dE}\, y_2 - y_3, \tag{14}$$

where the non-dimensional rate constants κ_{de} and κ_{dE} are related to k_i as:

$$\kappa_{de} = \frac{k_D\, k_{de}}{k_e^2}, \tag{15}$$

$$\kappa_{dE} = \frac{k_{dE}}{k_e}. \tag{16}$$

The whole system depends now on only two parameters, κ_{de} and κ_{dE}, making the analysis of its behaviour in the whole parameter space tractable. The system of equations (12)–(14) has two steady states ($\dot{y}_i = 0$), with only one of them being positive: $y_{1s} = y_{2s} = \left(-1 \pm \sqrt{1 + 8\kappa_{de}/\kappa_{dE}}\right)\Big/(4\kappa_{de})$,

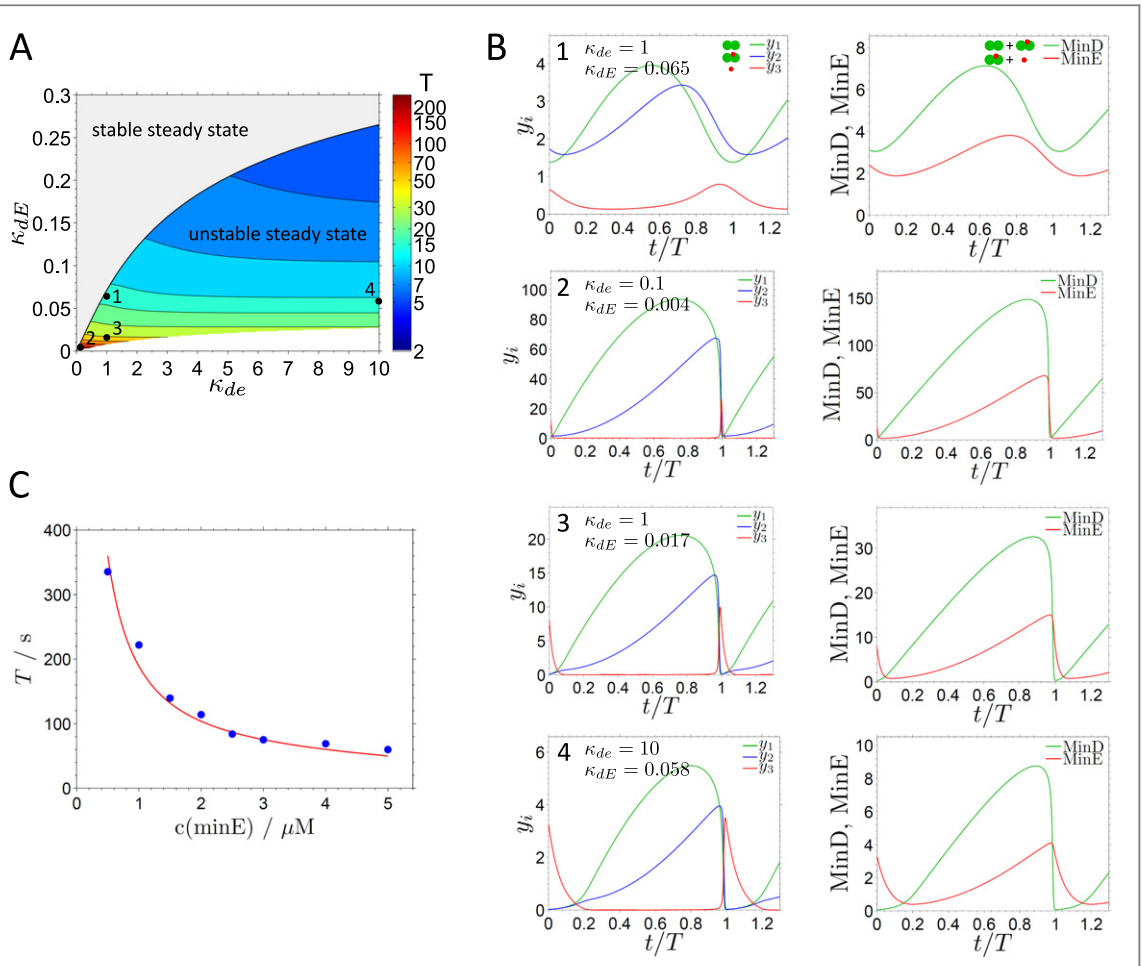

Figure 2. Solutions of the model M_{e2}, equations (12)–(14). A: the stability diagram showing the period T of the oscillatory solutions in the unstable region. B: the concentration oscillations of the three reacting species and the total MinD and MinE for several representative values of κ_{de} and κ_{dE}, as marked in A. C: the fit of the period dependence on κ_{dE} for $\kappa_{de} = 1$ ($T(\kappa_{dE})$, red line) to the dependence of the period of Min waves on the MinE bulk concentration, derived from the experimental data in [14] (blue points).

$y_{3s} = \kappa_{dE}\left(-1 \pm \sqrt{1 + 8\kappa_{de}/\kappa_{dE}}\right)/(2\kappa_{de})$. Linear stability analysis shows that the positive steady state can be either stable or unstable, depending on the values of κ_{de} and κ_{dE} (figure 2(A)). The steady state is unstable in the region of relatively large κ_{de} and relatively small κ_{dE}. In other words, a stable state can be made unstable by increasing κ_{de} or decreasing κ_{dE}, within the parameter range in figure 2(A). This points to the importance of the presence of MinE on the membrane for the instability: the reactions (3) and (5) in which the membrane-bound MinE participates must proceed with sufficiently high rate compared to the reactions (2) and (4) (MinE binding from the bulk) for the system to become unstable.

When the steady state is unstable, the system exhibits periodic oscillations of the concentrations y_i of all three species. The oscillations are close to sinusoidal near the bifurcation boundary (point 1 in figure 2(A), figure 2(B)), and increasingly deviate from this shape as one moves deeper into the unstable region of the parameter space (points 2–4). Although the concentration profiles vary with κ_{de} and κ_{dE}, they share common features: starting at the minimum of $MinD_2$, the concentration y_1 of $MinD_2$ increases, followed by a slower increase of the concentration y_2 of the $MinD_2$–MinE complex. The concentration y_3 of MinE increases only slowly, until it is at some point sufficiently high to overturn the trend of increasing y_1 through the reaction (3) and shortly thereafter to make y_2 decrease through the reaction (5). This reaction generates even more MinE on the membrane, leading to a sharp increase in y_3 and depletion of both y_1 and y_2. After the concentration of MinE decreases again due to spontaneous MinE detachment, the whole cycle can start again.

The depletion of the $MinD_2$–MinE complex and of the total MinE can occur extremely fast relative to the time window where all three concentrations increase (figures 2(A), (B), points 2 and 3). This behaviour persists when diffusion is added to the model, as shown below, and is also experimentally observed as a sharp edge of travelling Min waves [14]. In contrast, we could not find a set of parameters that would lead to similarly abrupt concentration changes in a model including autocatalytic attachment of MinD (model M_{dD} in figure 1(E)). Figure 3 shows the concentration oscillations in the model M_{dD} with a relatively steep decrease of MinE concentration. However, the difference between the overall rates of MinE concentration increase and decrease is

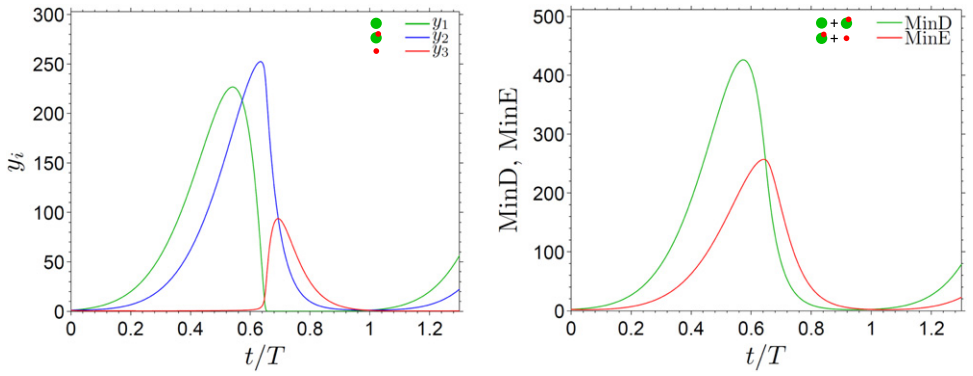

Figure 3. An oscillating solution of the autocatalytic MinD attachment model M_{dD} (figure 1(E)) with the rate parameters chosen so that the MinE depletion is faster relative to the MinE concentration increase. However, no parameter set could be found that would reproduce the strong asymmetry between the slow MinE concentration increase and its steep decrease as can be observed in the M_{e2} model (figure 2(B)). The parameter values are: $\kappa_{de} = \kappa_{d1} = \kappa_{dD} = 1$ and $\kappa_{dE} = 0.21$.

much less pronounced than in the model M_{e2} or in the experimentally observed Min waves (figure 6(E)). This failure to reproduce the sharp MinE decrease appears to be a typical feature of the models relying on the autocatalytic MinD attachment [14, 27].

Figure 2(A) also shows the dependence of the oscillation period T on the rates κ_{de} and κ_{dE}. The rate κ_{dE} can be assumed to depend linearly on the concentration of bulk MinE. We can therefore compare the dependence $T(\kappa_{dE})$ of the period T on the rate κ_{dE} with the experimental dependence of the wave period on the bulk MinE concentration, published previously [14]. Fitting the experimental data to the calculated $T(\kappa_{dE})$ shows that the trend of $T(\kappa_{dE})$ in the model M_{e2} agrees very well with the data (figure 2(C)). The parameters of the fit are: $k_e = 0.3\ \mathrm{s}^{-1}$ and $k^{\star}_{dE} \equiv k_{dE}/c\,(\mathrm{MinE}) = 4.3 \times 10^{-3}\ \mu\mathrm{M}^{-1}\mathrm{s}^{-1}$. The rate $k_e = 0.3\ \mathrm{s}^{-1}$ implies a MinE residence time of 3.3 s, if detachment were the only process of removing MinE species. This is compatible with the reported membrane residence times of MinE [39] between 6 and 12 s, as these experiments cannot distinguish between MinE and $MinD_2$–MinE complexes, and include also the effect of MinE binding to $MinD_2$ (reaction (3)) and therefore a longer residence time on the membrane.

Effect of direct MinE membrane binding

In the model M_{e2} it is assumed that MinE binds to $MinD_2$ present on the membrane (reactions (2) and (4)) but is not able to bind to the membrane directly. It is interesting to consider the opposite situation, when MinE binds directly to the membrane, and only this membrane-bound MinE, not MinE from the solution, can bind to $MinD_2$ present on the membrane. Thus, the reactions (2) and (4) are replaced by direct MinE attachment:

$$\varnothing \xrightarrow[k_E]{+\mathrm{MinE}} \mathrm{MinE}. \tag{17}$$

Assuming rate constant k_E for the MinE binding to the membrane, we obtain the model M_E (the direct MinE membrane attachment model) as a mathematically simpler alternative to M_{e2} (figure 1(D)):

$$\dot{y}_1 = 1 - \kappa_{de}\, y_1 y_3, \tag{18}$$

$$\dot{y}_2 = \kappa_{de}\, y_1 y_3 - \kappa_{de}\, y_2 y_3, \tag{19}$$

$$\dot{y}_3 = \kappa_E - \kappa_{de}\, y_1 y_3 + \kappa_{de}\, y_2 y_3 - y_3, \tag{20}$$

where the non-dimensional form of k_E, $\kappa_E = k_E/k_D$ is used.

The system of equations (18–20) has only one steady state, which is positive: $y_{1s} = y_{2s} = 1/(\kappa_{de}\,\kappa_E)$, $y_{3s} = \kappa_E$. Figure 4(A) shows the results of linear stability analysis of the steady state in the two-dimensional parameter space (κ_{de}, κ_E). For κ_E values larger than 0.5 the steady state is stable, regardless of κ_{de}. At $\kappa_E < 0.5$, a region of unstable steady states and oscillatory solutions exists. The temporal profiles of the concentrations $y_i(t)$ of these oscillating solutions are qualitatively similar to those of the model M_{e2} (figure 4(C)).

As κ_E becomes lower, approximately coinciding with the white region in figure 4(A), the concentrations y_1 and y_2 reach unrealistically high maximum values, and the period T becomes very long. In reality, this behaviour would be prevented by saturation of the membrane surface with proteins. The unbounded growth in simplified models, such as M_E, can be eliminated by taking into account the finite number of binding sites at the membrane (that is, by including surface saturation), or by adding reverse reactions, which have been neglected so far [41]. Such modifications can in some cases turn the unstable steady state into stable. If we include

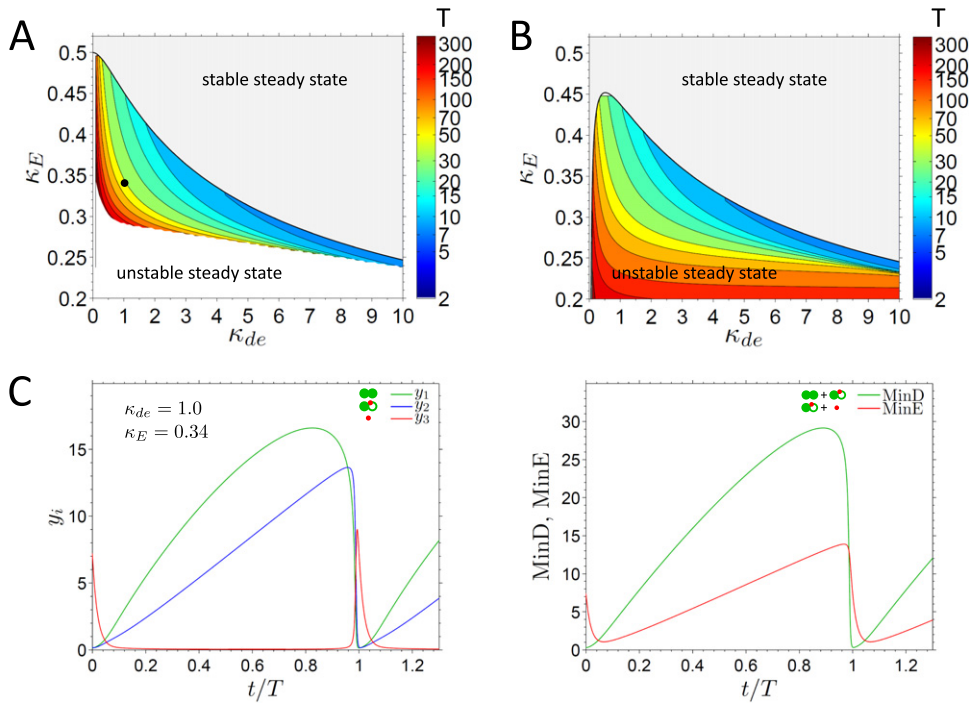

Figure 4. Solutions of the direct MinE membrane attachment model M_E. A: the stability diagram of the model M_E, equations (18)–(20). B: the stability diagram of the model M_E extended by adding spontaneous detachment of MinD with the rate constant $\kappa_d = 0.01$. C: the concentration oscillations of the three reacting species and the total MinD and MinE for $\kappa_{de} = 1$ and $\kappa_E = 0.34$ (the non-modified M_E model).

spontaneous detachment of $MinD_2$ from the membrane with the rate constant k_d, the steady state stays however unstable, and the concentrations of all species remain finite and within reasonable limits. This back-reaction of reaction (1) results in an additional term $-\kappa_d y_1$ in equation (18). The stability diagram with instability region extended in this way for a relatively small value of $\kappa_d = 0.01$ is shown in figure 4(B).

The comparison of models M_{e2} and M_E shows that the way MinE attaches to the membrane is not crucial for the existence of instabilities, and also for the basic characteristics of the shapes of the concentration profiles of the reacting species. It is therefore reasonable to speculate that the combination of the models M_{e2} and M_E, where both ways of MinE attachment to the membrane are allowed, would also display instability and similar concentration oscillations. This is relevant, because even though it is usually assumed that MinE does not bind directly to the membrane, there is experimental evidence that MinE can bind to the membrane weakly [42].

Effect of hydrolysis stimulation by a single MinE

The M_{e2} model assumes that the dissociation of the membrane $MinD_2$–MinE complex requires subsequent binding of two MinE to the MinD dimer. This requirement can be relaxed without destroying the instability of the steady state and losing the oscillatory behaviour.

Let us add the possibility that binding of the first MinE to the MinD dimer can be followed by hydrolysis of both ATPs, complex dissociation and detachment of MinD from the membrane. We combine all these reactions into a single step, described by the rate constant κ_{d1}:

$$\mathrm{MinD_2{-}MinE} \xrightarrow[k_{d1}]{-\mathrm{MinD_2}} \mathrm{MinE}. \qquad (21)$$

This reaction enters the model equations by adding the term $-\kappa_{d1} y_2$ to equation (13) and the term $+\kappa_{d1} y_2$ to equation (14). The system has now three steady states, only one of which is positive.

The $MinD_2$–MinE membrane complex can now disappear in essentially two ways: the newly added reaction (κ_{d1}) competes with the two reactions (4) and (5) requiring a second MinE (κ_{de}, κ_{dE}). The balance between the two groups of reactions affects the stability behaviour. The limiting case of κ_{de} and κ_{dE} dominating over κ_{d1} is the model M_{e2} analyzed above. The other extreme, κ_{d1} dominating over κ_{de} and κ_{dE}, leads to a stable steady state for all values of the remaining rate constants. In the intermediate cases there is an instability region, shrinking as κ_{d1} increases (figure 5).

This shows that even if not all of the $MinD_2$–MinE complex decays via reactions (4) and (5) the reaction system can be destabilized in a certain part of the parameter space.

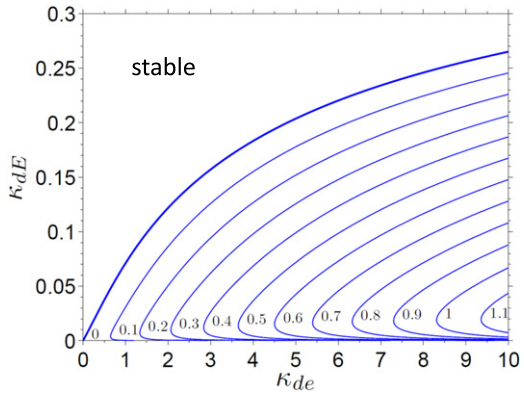

Figure 5. The stability diagram for the M_{e2} model extended by the possibility of a single MinE inducing the hydrolysis of both ATP molecules bound to the MinD dimer (rate κ_{d1}). The boundary between the stable and unstable regions is shown for κ_{d1} values between 0 and 1.1.

Including diffusion on infinite domain

So far we have considered a well-mixed chemical system without spatial coordinates. Finite diffusion prevents efficient mixing of the reacting species and can in general lead to inhomogeneous concentrations and formation of spatial patterns. The obvious questions one might ask are: can the system of chemical reactions in the model M_{e2}, together with finite diffusion, exhibit travelling wave patterns as observed in the experiments on supported membranes [14], and how similar are the shapes of these waves in the simple model M_{e2} to the experimental waves?

To account for diffusion, the diffusion terms with generally different diffusion coefficients D_i are added to the reaction equations (18)–(20):

$$\dot{y}_1 = 1 - \kappa_{de}\, y_1 y_3 - \kappa_{dE}\, y_1 + D_1 \Delta y_1, \tag{22}$$

$$\dot{y}_2 = \kappa_{de}\, y_1 y_3 + \kappa_{dE}\, y_1 - \kappa_{de}\, y_2 y_3 - \kappa_{dE}\, y_2 + D_2 \Delta y_2, \tag{23}$$

$$\dot{y}_3 = -\kappa_{de}\, y_1 y_3 + \kappa_{de}\, y_2 y_3 + 2\kappa_{dE}\, y_2 - y_3 + D_3 \Delta y_3, \tag{24}$$

We consider one-dimensional space, and look for periodic travelling wave solutions in form $y_i(x, t) = y_i(t - x/v)$ propagating with velocity v. This allows us to replace the space derivatives with time derivatives:

$$\dot{y}_1 = 1 - \kappa_{de}\, y_1 y_3 - \kappa_{dE}\, y_1 + b_1 \ddot{y}_1 \tag{25}$$

$$\dot{y}_2 = \kappa_{de}\, y_1 y_3 + \kappa_{dE}\, y_1 - \kappa_{de}\, y_2 y_3 - \kappa_{dE}\, y_2 + b_2 \ddot{y}_2 \tag{26}$$

$$\dot{y}_3 = -\kappa_{de}\, y_1 y_3 + \kappa_{de}\, y_2 y_3 + 2\kappa_{dE}\, y_2 - y_3 + b_3 \ddot{y}_3, \tag{27}$$

where we defined $b_i \equiv D_i/v^2$. Further, we express the diffusion coefficients D_2 and D_3 via D_1 by defining: $p_2 \equiv D_2/D_1$ and $p_3 \equiv D_3/D_1$. In the following, it is assumed for simplicity that the diffusion coefficients of $MinD_2$ and $MinD_2$–MinE complex on the membrane are equal: $p_2 = 1$. The system of equations (25)–(27) contains then two additional dimensionless parameters, b_1 and p_3, in comparison to the system without diffusion (equations (12)–(14)).

The parameters b_i can be understood as a relative measure of diffusion speed compared to the wave propagation velocity. Low b_i means small dispersion of molecules due to diffusion compared to the propagation of the phase of the wave over the intrinsic time scale of the reaction–diffusion system (determined by the reaction rates), and therefore a weak effect of mixing due to diffusion.

Solving equations (25)–(27) numerically gives a periodic wave solution for every value of b_i. This means that for a fixed values of the reaction rates and the diffusion coefficients D_i there is a range of solutions with different propagation velocities v and wavelengths $\lambda = vT$. The parameters of the propagating wave are therefore not determined uniquely.

Some solutions can be excluded on basis of their stability with respect to small perturbations: in unstable solutions even the smallest perturbations will grow, eventually causing the system to converge to a stable solution. In two dimensions the waves are usually circular or spiral, and only approximately planar; the stability conditions are therefore likely to differ from the 1D case considered here. Nevertheless, investigating the stability of solutions in 1D still provides important insights. Linear stability analysis of equations (22)–(24) identified a region in the space of the parameters b_1 and p_3 where the solutions are stable (figure 6(A)). In general, the waves

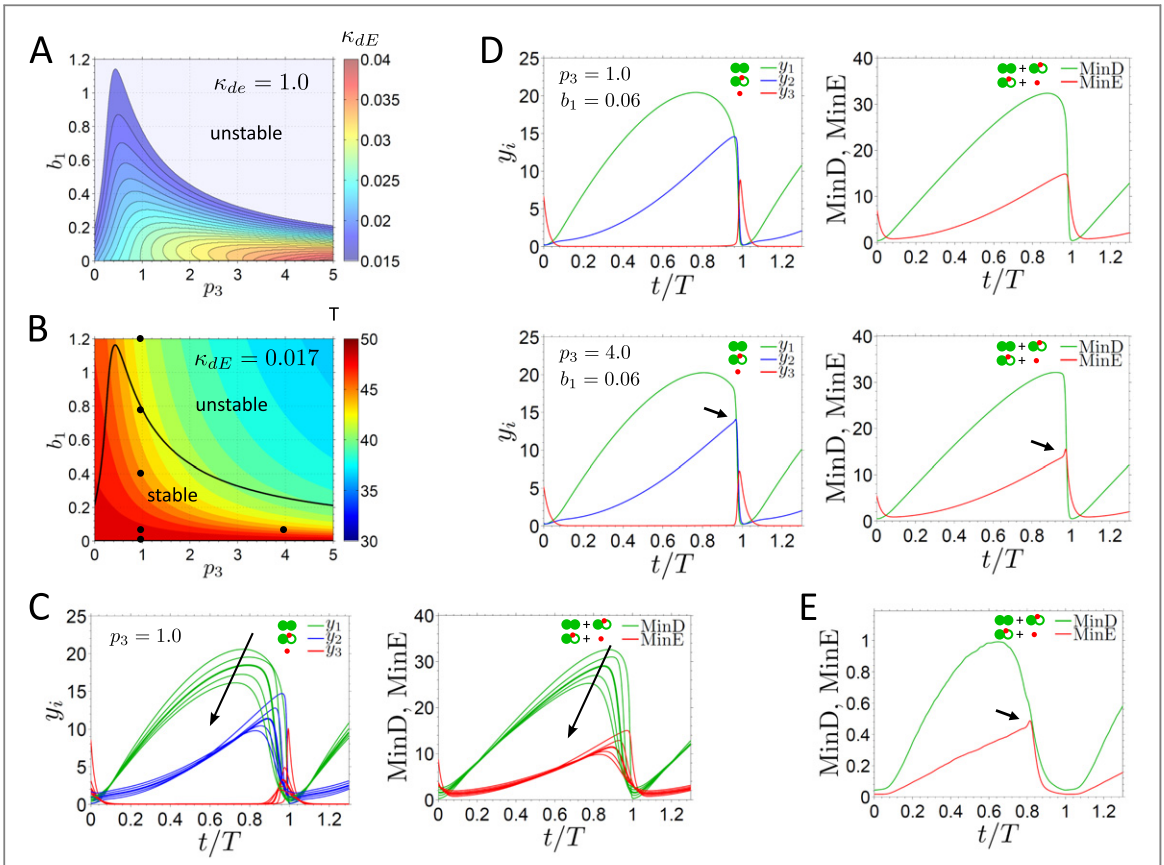

Figure 6. Travelling wave solutions of the reaction–diffusion model, equations (25)–(27). A: the stability diagram for $\kappa_{de} = 1$ and $\kappa_{dE} = 0.017$–0.040; the stable region shrinks with increasing κ_{dE}. B: the variation of the wave period T with b_1 and p_3 for $\kappa_{de} = 1$ and $\kappa_{dE} = 0.017$. C: the wave profiles for $p_3 = 1$ (i.e., $D_1 = D_3$) and $b_1 = 0, 0.4, 0.78, 1.2$ and 1.6 (in the direction of the arrow). The thick profiles correspond to the waves at the bifurcation point $b_1 = 0.78$. D: the wave profiles for $p_3 \equiv D_3/D_1 = 1$ and 4. The arrows indicate the sharp maxima of $MinD_2$–MinE and MinE concentrations. E: the experimental concentration profiles of MinD and MinE planar waves; adapted from [39].

are stable for small values of b_i, that is, for large propagation velocity and wavelength. The size of the stability region depends on the rate constants of the chemical reactions; for a fixed value of κ_{de} it becomes larger with decreasing κ_{dE}. The Min dynamics are spatially synchronized into coherent waves due to diffusional coupling. In the stable region, this coupling is not strong enough to destabilize the waves through strong mixing, which would otherwise lead to a homogeneous oscillating state.

Even though the solutions in the unstable region can be excluded, there is still a broad range of stable solutions that could in principle be realized. The experimentally observed Min waves on supported bilayers sometimes exhibit variations of wavelengths within one sample [43], although in many cases this range is rather narrow. Other chemical reaction–diffusion systems commonly show a broad range of wavelengths in different parts of the same sample and at the same time [44]. The experimental waves are likely to be to some extent influenced by the boundary conditions imposed by the sample container, and by the initial condition defined by the way the wave was initiated. In experiments, one strives to minimize the effects of these factors by using a large membrane area and by introducing a sufficient delay between the wave initiation and observation.

The period T of the waves depends rather weakly on b_1 and p_3 (figure 6(B)), in comparison with its dependence on the rates κ_{de} and κ_{dE} (figure 2(A)). One can therefore state that the wave period T is determined predominantly by the reaction part of the system.

The temporal (or equivalently, spatial) concentration profiles of the Min proteins vary with both b_i and p_3 (figure 6(C) and (D)). For a fixed value of $p_3 = 1$ the waves at small b_1 ($b_1 \to 0$) approach the concentration profiles in the absence of diffusion. With increasing b_1, that is, with decreasing velocity and also wavelength, the wave maxima and the wave modulation depth (the relative difference between the concentration minima and maxima) decrease. On the boundary between the stable and unstable regions, the wave modulation is still relatively high (more than 85% for the concentration profiles shown in thick lines in figure 6(C)). This is in agreement with the observed fact that the experimental Min waves exhibit deep modulation, that is, relatively high contrast between the concentration minima and maxima [14, 15, 39, 43].

The MinE molecule is smaller than the MinD dimer or the $MinD_2$–MinE complex; it is therefore interesting to consider the situation when MinE diffuses faster on the membrane than the other two species ($p_3 > 1$). Figure 6(D) compares the Min concentration profiles for equal diffusion of all three species ($p_3 = 1$) and for faster MinE diffusion ($p_3 = 4$). When MinE diffuses faster, the concentration profile y_2 of the $MinD_2$–MinE complex and, more dramatically, the total MinE concentration ($y_2 + y_3$) exhibit a sharp narrow maximum before a steep decay. Such a sharp peak near the falling edge of the MinE wave on a supported bilayer is indeed observed experimentally [14, 39] (figure 6(E)), and is reminiscent of the MinE ring observed in cells [45].

Observing the MinE reactions around the narrow peak of MinE (y_3, red curve in figure 6(D)) provides an insight into the mechanism of the Min wave propagation: at the falling edge of the MinE peak the dominant reaction of MinE is its detachment from the membrane (reaction (6)). Contrary to this, at the rising edge of the MinE peak the concentration of $MinD_2$–MinE is high, leading to net production of new MinE mainly via the reaction (5). The balance between these processes at the rising and falling edges of the MinE peak results in a peak of stable shape moving in the direction of high $MinD_2$–MinE concentration. The localized MinE peak (or a line, in 2D) resembles a propagating dissipative soliton [46].

Bounded domain with finite pool of reactants

The main differences between the conditions of oscillating Min patterns within living cells of *E. Coli* and the Min waves on supported lipid bilayers are the closed membrane geometry of the cell and the constant total number of reacting Min molecules in the cell. As an approximation of the situation in a living cell we consider here the reaction–diffusion model from the previous section with two modifications: first, the one-dimensional domain has a finite length L, with reflective boundary conditions for all three species: $\partial y_i(x, t)/\partial x = 0$. Second, the total numbers of MinE and MinD molecules on the membrane and in the bulk solution are constant.

The reaction–diffusion system of equations (22)–(24) then becomes:

$$\dot{y}_1 = \left(1 - \frac{d_s}{d_t}\right) - \kappa_{de}\, y_1 y_3 - \kappa_{dE}\left(1 - \frac{e_s}{e_t}\right) y_1 \qquad + D_1 \Delta y_1, \tag{28}$$

$$\dot{y}_2 = \kappa_{de}\, y_1 y_3 + \kappa_{dE}\left(1 - \frac{e_s}{e_t}\right) y_1 - \kappa_{de}\, y_2 y_3 - \kappa_{dE}\left(1 - \frac{e_s}{e_t}\right) y_2 + D_2 \Delta y_2, \tag{29}$$

$$\dot{y}_3 = -\kappa_{de}\, y_1 y_3 + \kappa_{de}\, y_2 y_3 + 2\kappa_{dE}\left(1 - \frac{e_s}{e_t}\right) y_2 - y_3 + D_3 \Delta y_3, \tag{30}$$

where d_t and e_t are the total numbers of MinD dimers and MinE molecules, respectively, and $d_s(t)$ and $e_s(t)$ are the surface-bound numbers of $MinD_2$ and MinE, respectively:

$$d_s = \int_0^1 \left(y_1 + y_2\right) \mathrm{d}x, \qquad e_s = \int_0^1 \left(y_2 + y_3\right) \mathrm{d}x. \tag{31}$$

The lengths x are expressed in the units of the domain length L; the integrals in equation (31) therefore cover the whole domain. Consequently, the units of the diffusion coefficients are $L^2 k_e$.

Since the parameter space became rather large through the addition of two more parameters (d_t and e_t) we did not perform a detailed analysis of equations (28)–(30) but present here a few numerical solutions relevant for the comparison with the published experimental findings. The following parameter values were used: $\kappa_{de} = 1$, $\kappa_{dE} = 0.017$, $D_1 = D_2 = 3 \times 10^{-5}$, $p_3 = 4$, $d_t = 12$ and $e_t = 8$. These non-dimensional values can result, for example, from the following parameters equations (10), (11), (15), (16): $k_D = 100$ p $\mu\mathrm{m}^{-1}\mathrm{s}^{-1}$, $k_{de} = 9 \times 10^{-4}$ $\mathrm{p}^{-1}\,\mu\mathrm{m}\,\mathrm{s}^{-1}$, $k_e = 0.3\ \mathrm{s}^{-1}$, $k_{dE} = 5.1 \times 10^{-3}\ \mathrm{s}^{-1}$, $D_{1,2} = 9 \times 10^{-4}\ \mu\mathrm{m}^2\,\mathrm{s}^{-1}$, $D_3 = 3.6 \times 10^{-3}\ \mu\mathrm{m}^2\,\mathrm{s}^{-1}$, $L = 10\ \mu$m, $c(\mathrm{MinD_2}) = 400$ p $\mu\mathrm{m}^{-1}$ and c (MinE) $= 267$ p $\mu\mathrm{m}^{-1}$, where 'p' stands for 'particle' and the one-dimensional concentrations are expressed in 'particles per μm'.

Setting D_1 to $D_1 = 3 \times 10^{-5}$ resulted in oscillations of Min proteins between the two ends of the domain, reminiscent of the pole-to-pole oscillations observed in cells (figure 7(A)): the concentration of Min proteins builds up in one half of the domain; upon reaching a certain level the molecules suddenly detach, starting near the middle and progressing towards one end; and at the same time the population of molecules on the membrane in the other half of the domain starts to increase.

A closer look at the concentration profiles of all three species (figure 7(B)) shows that the wave progressing from the center towards the end of the domain is similar to the travelling waves on infinite domain (figure 6(D)). Interestingly, the wave always propagates from the center towards the alternating ends, not from one end towards the other. This behaviour is known from living cells [13] and synthetic enclosed compartments [19], but is not observed on finite membrane patches with unlimited supply of Min molecules [16].

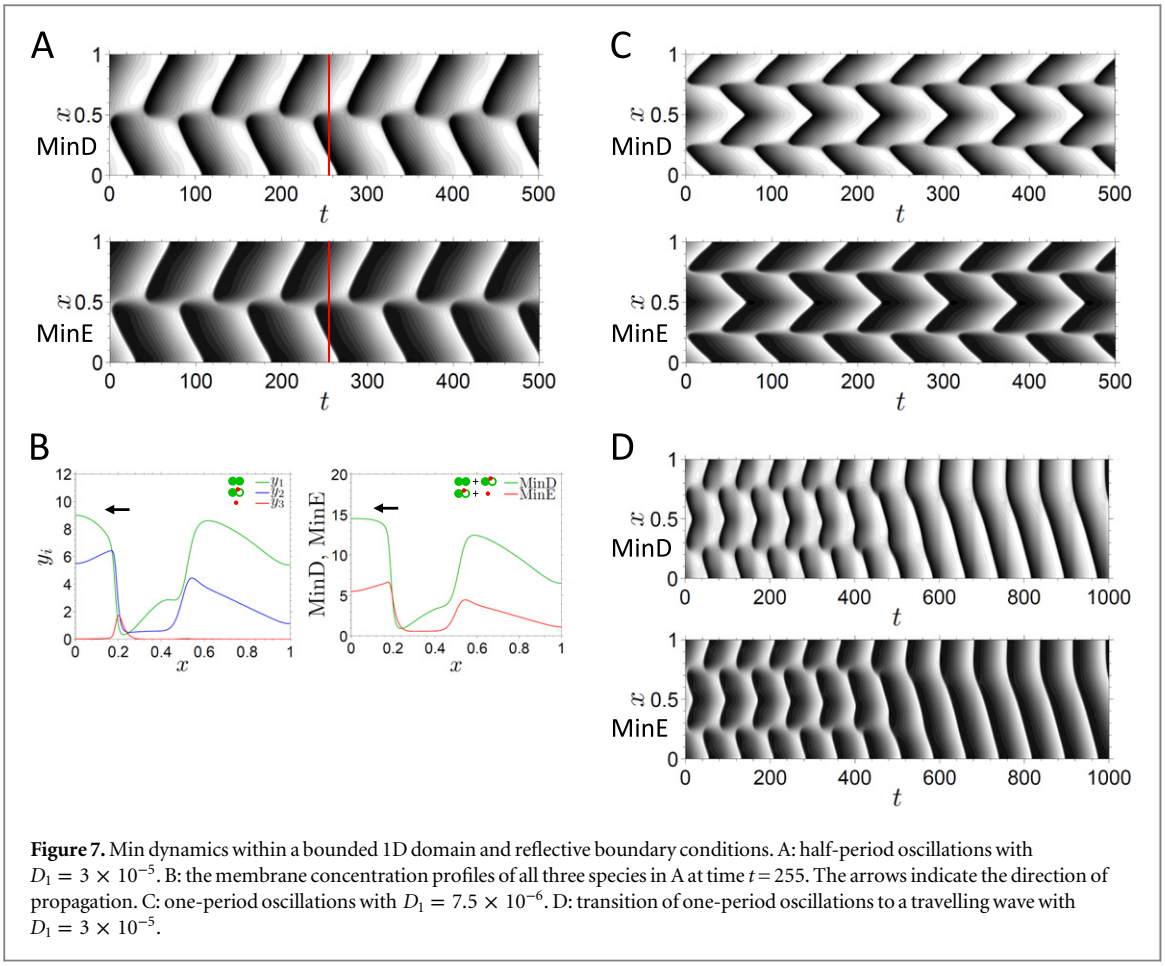

Figure 7. Min dynamics within a bounded 1D domain and reflective boundary conditions. A: half-period oscillations with $D_1 = 3 \times 10^{-5}$. B: the membrane concentration profiles of all three species in A at time $t = 255$. The arrows indicate the direction of propagation. C: one-period oscillations with $D_1 = 7.5 \times 10^{-6}$. D: transition of one-period oscillations to a travelling wave with $D_1 = 3 \times 10^{-5}$.

In long filamentous cells [27, 47] and in long artificial enclosed microcompartments [19], a standing-wave-like pattern with the number of nodes depending on the cell length has been observed experimentally. This pattern can be thought of as composed of several oscillating short-cell patterns aligned along each other. The periodic oscillation between the two cell poles in the shortest cells corresponds to one half of the wavelength of the patterns in the long cells.

Because of the reflective boundary condition, the same effect can be obtained with the system of equations (28)–(30): doubling the domain length L, or equivalently, reducing the diffusion coefficient by a factor of four, allows solutions with one period per domain length (figure 7(C)). Depending on the exact value of D, this pattern may become unstable, converting into a travelling-wave pattern (figure 7(D)), which appears to be stable. A similar travelling-wave pattern has been observed in longer cells [27].

Transitions from one stable oscillating pattern to another as the domain length slowly increases are observed in growing cells before the division. The likely explanation is that the initially stable pattern becomes unstable with longer domain length and converts to a new stable state. The initial state in figure 7(D) is however unstable for the used parameters, because no change of domain length or perturbation was necessary to induce the transition to a different pattern. Transitions between two stable patterns without any changes of parameters have been observed in particle-based simulations of the Min dynamics in two dimensions [48]. This result points to the importance of stochastic fluctuations for the conversion between stable patterns separated by an unstable region, a phenomenon not directly revealed by deterministic models.

The Min dynamics shown in figure 7(A) and (C) can be viewed as waves propagating in alternating directions. The wave propagates until it collides with the boundary or annihilates with another wave travelling towards it; in its wake a new wave emerges, moving in the opposite direction. It appears that in closed-volume geometries where the supply of bulk Min proteins is limited this dynamics is preffered to waves travelling in the same direction. Indeed, this is the predominant behaviour observed in short cells [13] and in enclosed compartments [19], in long filamentous cells [27, 47], and even in larger 2D compartments where the total volume is limited by their small height [49].

Discussion

In this work we explored simple one-dimensional models of Min dynamics that consider only the species and reactions on the membrane, and do not contain direct autocatalytic reactions.

In living cells, the supply of Min molecules in the bulk is limited, therefore it is conceivable that bulk reactions, such as conversion of MinD–ADP to MinD–ATP, could be a vital part of the reaction system underlying the Min oscillations. However, Min proteins exhibit complex dynamics also when the supply of Min molecules is virtually infinite, as the experiments with wave patterns on supported lipid bilayers show [15, 39]. The fast protein diffusion in the solution above the membrane in relation to the speed of the propagating waves in these experiments guarantees substantial mixing of the bulk solution on the relevant time scales. Although reactions and diffusion in bulk may still influence the observed patterns, as suggested by experiments [16] and theoretical work [27], they are unlikely to be the decisive factor behind the Min dynamics. It is further reasonable to assume that the molecular mechanism of the Min dynamics in cells and on the planar bilayers is the same. For these reasons we considered only reactions and diffusion on the membrane.

Experiments show that the concentration of membrane-bound MinD increases more than linearly with the concentration of the MinD in solution [36, 50]. There is, however, no evidence that this happens as a consequence of an autocatalytic binding process as it is commonly implemented in the models [16, 26, 27]. Similar nonlinear increase could be caused, for example, by MinD aggregation on the membrane following simple membrane binding. As noted before [24], this type of aggregation is, however, not sufficient to generate instabilities of the steady state leading to the observed Min behaviour. Furthermore, the autocatalytic binding would have to be a complex process with at least two steps: transient interaction (binding) of the membrane-bound and bulk MinD (since one promotes membrane binding of the other), and subsequent dissociation of this complex into two membrane-bound MinD molecules. Although this process can in principle take place, it is certainly worth inspecting alternative Min models that do not rely on its existence.

The models presented here are relatively simple in comparison with other suggested models of Min dynamics. All of them have three reacting species. This is the minimum number: it has been shown that systems with only two reactants and at most bimolecular reactions cannot show limit-cycle oscillations [51]. Wilhelm [33] identified the smallest chemical reaction system that exhibits instability via Hopf bifurcation. The models M_{e2} and especially the direct MinE membrane attachment model M_{E} are close to this minimal system in terms of their complexity, defined in terms of the number of reactive species, the number of total and bimolecular reactions and the number of quadratic terms in the reaction equations.

The Wilhelm's model contains an autocatalytic term; its instability can however be traced to a negative feedback loop. Contrary to the autocatalytic MinD attachment model M_{dD}, the models M_{e2} and M_{E} have no direct autocatalytic term, it is therefore interesting to see if it is possible to pinpoint the cause of their instability.

The origins of instability in chemical reaction systems have been classified by Tyson [52]. This classification is based on the Jacobian matrix $\{a_{ij}\} = \partial F_i / \partial y_j$ of the chemical reaction system $\dot{y}_i = F_i(y_j)$. For the steady state to be qualitatively stable (meaning stable regardless of the parameter values) the sign pattern of the Jacobian matrix in the steady state has to fulfil several conditions. These conditions guarantee that the eigenvalues of the Jacobian matrix have negative real parts, that is, that any perturbation of the steady state dies out. The unstable steady states are classified depending on the stability conditions that are violated.

The steady-state sign patterns of the Jacobian matrices for the three models considered here (figure 1) are:

$$\mathrm{M}_{e2},\ M_E: \quad \begin{pmatrix} - & 0 & - \\ + & - & 0 \\ - & + & - \end{pmatrix}, \qquad \mathrm{M}_{dD}: \quad \begin{pmatrix} - & 0 & - \\ + & - & + \\ - & + & - \end{pmatrix}. \tag{32}$$

The models M_{e2} and M_{E} have two destabilizing elements: a negative feedback loop: $\mathrm{MinD}_2 \rightarrow \mathrm{MinD}_2$–$\mathrm{MinE} \rightarrow \mathrm{MinE} \dashv \mathrm{MinD}_2$ ($a_{21}a_{13}a_{32} < 0$) and an indirect autocatalysis (competition): $\mathrm{MinD}_2 \dashv \mathrm{MinE} \dashv \mathrm{MinD}_2$ ($a_{13}a_{31} > 0$). The model M_{dD} has additionally another indirect autocatalysis (symbiosis): $\mathrm{MinE} \rightarrow \mathrm{MinD}_2$–$\mathrm{MinE} \rightarrow \mathrm{MinE}$ ($a_{23}a_{32} > 0$). This third destabilizing factor can also appear in the model M_{e2} if the approximation of equal rate constants of the reaction pairs (2)–(4) and (3)–(5) is not made.

Since there are two or even three violated stability conditions, it is not possible to identify a single reaction or an element of these models as a sole reason for the instability. It is, however, interesting to note that the direct autocatalysis of MinD in the model M_{dD} is not one of the destabilizing elements, since $a_{11} < 0$. In other words, in the steady state of the model M_{dD}, an infinitesimal increase of MinD concentration will induce its decrease back towards the steady state value and not further away from it, as the autocatalytic attachment term might seem to suggest. This happens because the combined rates of the two MinE-attachment reactions (reactions (2) and (4), both decreasing the MinD concentration) will increase more strongly than the autocatalytic MinD attachment (increasing the MinD concentration). The presence of the MinE species on the membrane and its

bimolecular interaction with MinD appears therefore to be more relevant for the Min dynamics than the mode of MinD attachment (plain or autocatalytic) to the membrane.

The model M_{e2} inintroduced here leads to concentration profiles of Min proteins qualitatively similar to those observed on supported lipid bilayers. Most importantly, it reproduces the sharp concentration decrease at the end of the wave, and even the narrow sharp maximum of MinE preceding this decrease. It also agrees with the experimental dependence of the wave period T on the bulk MinE concentration. The rate constant of MinE detachment from the membrane k_e obtained from the fit to these data is consistent with other experimental data.

An important feature of the model is its robustness to modifications. It appears not to be particularly important how MinE reaches the membrane—either by binding to membrane-bound MinD or by direct binding—the existence of instability and the general shapes of the profiles are not affected. Also the assumption that two MinE molecules are required to induce MinD detachment from the membrane is not absolute; the instability is preserved even if this is only one of the possible pathways.

The model also exhibits qualitatively similar dynamics to those in living cells when formulated for finite interval and constant total number of Min molecules. The difference between the model solutions and the oscillation patterns observed in cells [53] can possibly be linked to the rather crude approximation of the full 3D cell geometry by the one-dimensional interval. For a typical cell shape, the hemispherical end cups closing the cylindrical cell volume, completely ignored in the 1D approximation, can amount to more than 1/3 of the total membrane surface.

The reduction of dimensionality to 1D is also relevant for the dynamics on infinite domain: while the results shown in figure 6 may provide a good description of the spiral waves far from the spiral center, where they can be locally well approximated by a planar wave, the 1D model cannot accurately describe the two-dimensional center of the spiral. When using 1D approximation, particularly when dealing with finite domains, solutions that cannot be simply reduced to one dimension may exist in the original dimension [24], and the patterns stable in 1D approximation may become unstable in higher dimensions due to the existence of additional perturbation modes.

An obvious extension of this work is the solution of the presented model in various 3D geometries: normal and filamentous cell shapes, and synthetic compartments of different aspect ratios. Exploring the theoretical dependence of the wave parameters (period, wavelength, the shape of the concentration profile) on the Min protein concentrations, membrane diffusion coefficients and membrane binding affinities will provide predictions that can be tested experimentally. These experiments will ultimately show whether the proposed interaction of two MinE molecules with MinD before the detachment of MinD from the membrane is indeed the key factor behind the Min dynamics.

References

[1] Cross M C and Hohenberg P C 1993 Pattern formation outside of equilibrium *Rev. Mod. Phys.* **65** 851–1112
[2] Field R J and Noyes R M 1974 Oscillations in chemical systems: IV. Limit cycle behavior in a model of a real chemical reaction *J. Chem. Phys.* **60** 1877–84
[3] Nicolis G and Portnow J 1973 Chemical oscillations *Chem. Rev.* **73** 365–84
[4] Koch A J and Meinhardt H 1994 Biological pattern formation: From basic mechanisms to complex structures *Rev. Mod. Phys.* **66** 1481–507
[5] Goldbeter A, Gerard C, Gonze D, Leloup J-C and Dupont G 2012 Systems biology of cellular rhythms *FEBS Lett.* **586** 2955–65
[6] Meinhardt H 2012 Turing's theory of morphogenesis of 1952 and the subsequent discovery of the crucial role of local self-enhancement and long-range inhibition *Interface Focus* **2** 407–16
[7] Turing A M 1952 The chemical basis of morphogenesis *Phil. Trans. R. Soc.* B **237** 37–72
[8] Lawrence P A and Struhl G 1996 Morphogens, compartments, and pattern: lessons from Drosophila? *Cell* **85** 951–61
[9] Kondo S and Miura T 2010 Reaction–diffusion model as a framework for understanding biological pattern formation *Science* **329** 1616–20
[10] Bell-Pedersen D, Cassone V M, Earnest D J, Golden S S, Hardin P E, Thomas T L and Zoran M J 2005 Circadian rhythms from multiple oscillators: lessons from diverse organisms *Nat. Rev. Genetics* **6** 544–56
[11] Goldbeter A 1995 A model for circadian oscillations in the Drosophila period protein (PER) *Proc. R. Soc.* B **261** 319–24
[12] Lutkenhaus Joe 2007 Assembly dynamics of the bacterial MinCDE system and spatial regulation of the Z ring *Annu. Rev. Biochem.* **76** 539–62
[13] Shih Y-L and Zheng M 2013 Spatial control of the cell division site by the Min system in *Escherichia coli Environ. Microbiol.* **15** 3229–39
[14] Loose M, Fischer-Friedrich E, Ries J, Kruse K and Schwille P 2008 Spatial regulators for bacterial cell division self-organize into surface waves *in vitro Science* **320** 789–92
[15] Ivanov V and Mizuuchi K 2010 Multiple modes of interconverting dynamic pattern formation by bacterial cell division proteins *Proc. Natl Acad. Sci. USA* **107** 8071–8
[16] Schweizer J, Loose M, Bonny M, Kruse K, Mönch I and Schwille P 2012 Geometry sensing by self-organized protein patterns *Proc. Natl Acad. Sci. USA* **109** 15283–8
[17] Zieske K, Schweizer J and Schwille P 2014 Surface topology assisted alignment of Min protein waves *FEBS Lett.* **588** 2545–9
[18] Martos A, Petrášek Z and Schwille P 2013 Propagation of MinCDE waves on free-standing membranes *Environ. Microbiol.* **15** 3319–26
[19] Zieske K and Schwille P 2013 Reconstitution of pole-to-pole oscillations of Min proteins in microengineered polydimethylsiloxane compartments *Angew. Chem., Int. Ed. Engl.* **52** 459–62

[20] Meinhardt H and de Boer P A J 2001 Pattern formation in *Escherichia coli*: a model for the pole-to-pole oscillations of Min proteins and the localization of the division site *Proc. Natl Acad. Sci. USA* **98** 14202–7
[21] Howard M, Rutenberg A D and de Vet S 2001 Dynamic compartmentalization of bacteria: Accurate division in E. Coli *Phys. Rev. Lett.* **87** 278102
[22] Kruse K 2002 A dynamic model for determining the middle of *Escherichia coli Biophys. J.* **82** 618–27
[23] Meacci G and Kruse K 2005 Min-oscillations in *Escherichia coli* induced by interactions of membrane-bound proteins *Phys. Biol.* **2** 89–97
[24] Fischer-Friedrich E, Nguyen van yen R and Kruse K 2007 Surface waves of Min-proteins *Phys. Biol.* **4** 38–47
[25] Huang K C, Meir Y and Wingreen N S 2003 Dynamic structures in *Escherichia coli*: spontaneous formation of MinE rings and MinD polar zones *Proc. Natl Acad. Sci. USA* **100** 12724–8
[26] Arjunan S N V and Tomita M 2010 A new multicompartmental reaction–diffusion modeling method links transient membrane attachment of *E. coli* MinE to E-ring formation *Syst. Synth. Biol.* **4** 35–53
[27] Bonny M, Fischer-Friedrich E, Loose M, Schwille P and Kruse K 2013 Membrane binding of MinE allows for a comprehensive description of Min-protein pattern formation *PLoS Comput. Biol.* **9** e1003347
[28] Halatek J and Frey E 2012 Highly canalized MinD transfer and MinE sequestration explain the origin of robust MinCDE-protein dynamics. *Cell Rep.* **1** 741–52
[29] Tostevin F and Howard M 2006 A stochastic model of Min oscillations in *Escherichia coli* and Min protein segregation during cell division *Phys. Biol.* **3** 1–12
[30] Drew D A, Osborn M J and Rothfield L I 2005 A polymerization-depolymerization model that accurately generates the self-sustained oscillatory system involved in bacterial division site placement *Proc. Natl Acad. Sci. USA* **102** 6114–8
[31] Cytrynbaum E N and Marshall B D L 2007 A multistranded polymer model explains MinDE dynamics in *E. coli* cell division *Biophys. J.* **93** 1134–50
[32] Sengupta S, Derr J, Sain A and Rutenberg A D 2012 Stuttering Min oscillations within *E. coli* bacteria: a stochastic polymerization model *Phys. Biol.* **9** 056003
[33] Wilhelm T and Heinrich R 1995 Smallest chemical reaction system with Hopf bifurcation *J. Math. Chem.* **17** 1–14
[34] Hu Z L, Gogol E P and Lutkenhaus J 2002 Dynamic assembly of MinD on phospholipid vesicles regulated by ATP and MinE *Proc. Natl Acad. Sci. USA* **99** 6761–6
[35] Hu Z L, Saez C and Lutkenhaus J 2003 Recruitment of MinC, an inhibitor of Z-ring formation, to the membrane in *Escherichia coli*: role of MinD and MinE *J. Bacteriol.* **185** 196–203
[36] Lackner L L, Raskin D M and de Boer P A J 2003 ATP-Dependent interactions between *Escherichia coli* Min proteins and the phospholipid membrane *in vitro J. Bacteriol.* **185** 735–49
[37] Hu Z L and Lutkenhaus J 2001 Topological regulation of cell division in *E coli*: spatiotemporal oscillation of MinD requires stimulation of its ATPase by MinE and phospholipid *Mol. Cell* **7** 1337–43
[38] Wu W, Park K-T, Holyoak T and Lutkenhaus J 2011 Determination of the structure of the MinD–ATP complex reveals the orientation of MinD on the membrane and the relative location of the binding sites for MinE and MinC *Mol. Microbiol.* **79** 1515–28
[39] Loose M, Fischer-Friedrich E, Herold C, Kruse K and Schwille P 2011 Min protein patterns emerge from rapid rebinding and membrane interaction of MinE *Nat. Struct. Mol. Biol.* **18** 577–83
[40] Park K-T, Wu W, Battaile K P, Lovell S, Holyoak T and Lutkenhaus J 2011 The Min oscillator uses MinD-dependent conformational changes in MinE to spatially regulate cytokinesis *Cell* **146** 396–407
[41] Schnakenberg J 1979 Simple chemical reaction systems with limit cycle behavior *J. Theor. Biol.* **81** 389–400
[42] Renner L D and Weibel D B 2012 MinD and MinE interact with anionic phospholipids and regulate division plane formation in *Escherichia coli J. Biol. Chem.* **287** 38835–44
[43] Vecchiarelli A G, Li M, Mizuuchi M and Mizuuchi K 2014 Differential affinities of MinD and MinE to anionic phospholipid influence Min patterning dynamics in vitro *Mol. Microbiol.* **93** 453–63
[44] Epstein I R and Showalter K 1996 Nonlinear chemical dynamics: oscillations, patterns, and chaos *J. Phys. Chem.* **100** 13132–47
[45] Hale C A, Meinhardt H and de Boer P A J 2001 Dynamic localization cycle of the cell division regulator MinE in *Escherichia coli Eur. Mol. Biol. J.* **20** 1563–72
[46] Vanag V K and Epstein I R 2007 Localized patterns in reaction–diffusion systems *Chaos* **17** 037110
[47] Raskin D M and de Boer P A J 1999 Rapid pole-to-pole oscillation of a protein required for directing division to the middle of *Escherichia coli Proc. Natl Acad. Sci. USA* **96** 4971–6
[48] Hoffmann M and Schwarz U S 2014 Oscillations of Min-proteins in micropatterned environments: a three-dimensional particle-based stochastic simulation approach *Soft Matter* **10** 2388–96
[49] Zieske K and Schwille P 2014 Reconstitution of self-organizing protein gradients as spatial cues in cell-free systems. *ELife* **3** 03949
[50] Mileykovskaya E, Fishov I, Fu X Y, Corbin B D, Margolin W and Dowhan W 2003 Effects of phospholipid composition on MinD-membrane interactions *in vitro* and *in vivo J. Biol. Chem.* **278** 22193–8
[51] Póta G 1983 Two-component bimolecular systems cannot have limit cycles: A complete proof *J. Chem. Phys.* **78** 1621–2
[52] Tyson J J 1975 Classification of instabilities in chemical reaction systems *J. Chem. Phys.* **62** 1010–5
[53] Fischer-Friedrich E, Meacci G, Lutkenhaus J, Chate H and Kruse K 2010 Intra- and inter-cellular fluctuations in Min-protein dynamics decrease with cell length *Proc. Natl Acad. Sci. USA* **107** 6134–9